Reprinted from:
1972, *Phys. Earth Planet. Interiors* **6**, 346–359. North-Holland Publishing Company, Amsterdam
Printed in the Netherlands

MECHANISM OF TSUNAMI EARTHQUAKES

HIROO KANAMORI

Earthquake Research Institute, Tokyo University, Tokyo, Japan

Received 24 April 1972

The mechanism of the Aleutian islands earthquake of 1946 and the Sanriku earthquake of 1896 is studied on the basis of the data on seismic waves from 5 to 100 s and on tsunamis. These earthquakes generated, despite their relatively small earthquake magnitude, two of the largest and most widespread tsunamis in history. The data obtained at different periods are interpreted in terms of the effective moment, M_e. The effective moment at a certain period is defined as a seismic moment of a virtual step function dislocation that explains the observation at this period. The effective moment of the tsunami earthquakes increases rapidly towards 0.5 to 1.0×10^{29} dyne · cm as the period increases while, for ordinary earthquakes, it is more or less constant. This dependence can be explained in terms of a source deformation having a time constant of about 100 s. The M_e versus f (frequency) diagram provides a diagnostic method of estimating the tsunami potential of earthquakes. If the M_e–f diagram for an earthquake has a steep upgrade towards low frequency implying an effective moment exceeding 10^{28} dyne · cm at zero frequency, the earthquake has a high tsunami potential. Since the determination of the effective moment at various periods can be made by a simple procedure, this method could be incorporated in the tsunami warning system. The abnormal slow deformation at the source of the tsunami earthquakes may be a manifestation of viscoelasticity of a weak zone beneath the inner margin of the trenches. The weak zone which is implied by large normal-fault earthquakes such as the 1933 Sanriku and the 1929 Aleutian islands earthquakes may be a result of frictional heating at the interface between the oceanic and the continental lithospheres.

1. Introduction

Among great tsunamis in history, two tsunamis, one originating in the Sanriku region, Japan, in 1896, and the other in the Aleutian region in 1946 (figs. 1 and 2), are very abnormal in the light of the ordinary concept of tsunami generation by earthquakes. Despite the unusual tsunami height, the earthquakes that set off these tsunamis are of only moderate magnitude. Although the instrumental data are inevitably very incomplete for the 1896 Sanriku event, macroseismic data such as the intensity distribution suggest that it was definitely not an exceptionally large earthquake, at least over the periods from 1 to 5 s. According to IKI (1896), inhabitants along the Sanriku coast, about 150 to 200 km away from the epicenter, felt, preceding the tsunami, only "slight to weak" (corresponding to M.M. scale of I to IV) shocks with relatively long duration. The tsunami was, nevertheless, devastating; waves as high as 30 m were observed along the Sanriku coast and as many as 27122 lives were lost (see IMAMURA, 1937, p. 128).

The 1946 Aleutian islands earthquake generated one of the largest and most widespread tsunamis in the Pacific during this century (GREEN, 1946; GUTENBERG and RICHTER, 1954). ADAMS (1971) considered it to be at least a "one per two-thousand years" event. The surface-wave magnitude of this event, however, is 7.4 (GUTENBERG and RICHTER, 1954) suggesting that it is only a moderate-size earthquake at least around the period of 20 s. BRUNE and ENGEN (1969) found that the excitation of 100 s surface waves by this event is relatively large; they assign this event a 100 s magnitude of 7.8. SYKES (1971) who found that the aftershock zone of this event is only 50 to 100 km long suggests that a relatively small rupture zone with an abnormally large average displacement appears to be an explanation of the large tsunami. However, the 100 s magnitude of 7.8 is not large enough to suggest immediately such a large displacement.

Thus the generating mechanisms of these two great tsunamis are still in question. We will call these unusual earthquakes "tsunami earthquakes" in the present paper.

This paper attempts to present the seismic-wave data from 5 to 100 s and the tsunami data in a unified

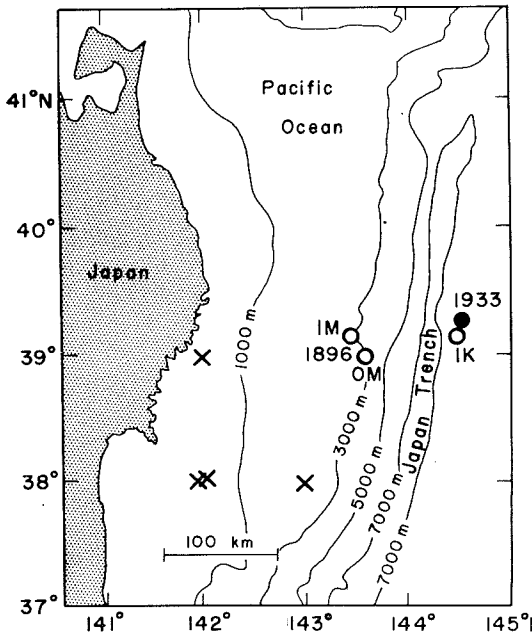

Fig. 1. The epicenters of the 1896 (open circle) and the 1933 (filled circle) Sanriku earthquakes. For the 1896 earthquake, the epicenters according to Imamura, Iki (reported in IMAMURA, 1899) and OMORI (1900) are indicated by IM, IK and OM respectively. OMORI's (1900) epicenter which is determined on the basis of the distribution of the seismic intensity is probably most reliable. The crosses indicate the aftershocks of the 1896 event (RICHTER, 1958).

scheme for the purpose of unravelling such an abnormal generating mechanism. It is hoped that this study contributes to the understanding of the physical properties of the mantle which is responsible for such a mechanism, and to the improvement of the tsunami warning system.

2. Method of analysis

The data on seismic body waves, 20 s surface waves, long-period Love and Rayleigh waves, and tsunamis constitute the basic data used in the present study. Seismic waves of a certain period convey the information of such component of the source displacement that has a time constant comparable to the period. The tsunami data carry the information of the source displacement having a longer time constant, probably up to 500 s or so. Combining the seismic-wave data and the tsunami data, we may envisage in detail the nature of the source displacement. In combining these different sets of data, however, one difficulty arises because the different kinds of data are usually interpreted in terms

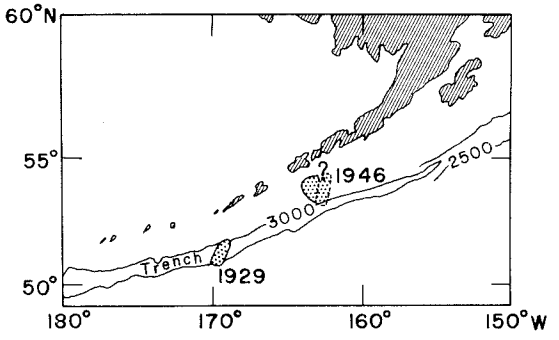

Fig. 2. The aftershock areas of the 1929 and the 1946 earthquakes in the Aleutians (according to SYKES, 1971). Water depths are given in fathoms.

of different physical parameters describing the "magnitude" of the source. The seismic body waves are usually interpreted in terms of the body-wave magnitude m_b, and the 20 s surface waves are interpreted in terms of the surface wave magnitude M_s; the longer period Love and Rayleigh waves are usually interpreted in terms of the seismic moment. The tsunami data are often interpreted in terms of the wave height at the tsunami source region. In order to remove this inconvenience we shall introduce a parameter, effective moment, and present the results from different sources in a unified scheme.

The effective moment is defined as follows. We let $D(t)$ represent the source shear dislocation. The moment $M(t)$ of the equivalent point source double couple is proportional to $D(t)$. If $D(t) = D_0 H(t)$ where $H(t)$ is the Heaviside step function and D_0 is the static dislocation, then the spectral density of $D(t)$ is $|\hat{D}(\omega)| = D_0/\omega$. The corresponding spectral density of the moment is $|\hat{M}(\omega)| = M_0/\omega$ where M_0 is the static moment. When the source process has a finite time constant τ, we have a source dislocation of the form $D(t;\tau)$ where $D(t;\tau) = 0$ for $t < 0$ and $D(\infty;\tau) = D_0$. If we write the amplitude spectral density of this type of dislocation as

$$|\hat{D}(\omega)| = D_e(\omega)/\omega$$

then $D_e(\omega)$ may be regarded as the height of a virtual step-function type dislocation that gives the same spectral density, at ω, as that of $D(t;\tau)$. In this sense, $D_e(\omega)$ may be termed the effective dislocation at ω. The moment corresponding to $D_e(\omega)$ is called the effective moment $M_e(\omega)$, i.e.

$$M_e(\omega) = \omega\,|\hat{M}(\omega)|.$$

2.1. *Conversion of body-wave magnitude to effective moment*

The body wave magnitude m_b at period T is related to the maximum amplitude A of a body wave train at an arbitrary reference distance Δ_r; the relations are given by the charts of GUTENBERG (1945) and RICHTER (1958). Since the body wave train $f(t)$ usually consists of two or three pulses, we may assume it to be of the form:

$$f(t) = 0 \qquad \text{for } t < 0,$$
$$f(t) = A \exp(-t/2T) \sin(2\pi t/T) \qquad \text{for } t \geq 0,$$

where T is the approximate period of the wave train and t is the time measured from the onset. The amplitude spectral density at $\omega = 2\pi/T$ then becomes

$$| \hat{U}_c(\omega) | = AT = 2\pi A/\omega, \tag{1}$$

which is probably correct within a factor of two or so. The subscript c stands for P or S depending upon the kind of the wave used in the determination of m_b. Thus, if the average body wave magnitude is known for an earthquake, we can convert it to the average amplitude spectral density $| \overline{\hat{U}_c(\omega)} |$ at an arbitrary reference distance Δ_r. The average spectral density $| \overline{\hat{U}_c(\omega)} |$ can be related to the effective moment by the standard technique which is outlined below.

In an infinite homogeneous elastic medium, the far-field displacement resulting from a double-couple point source with a moment $M(t)$ is given by (LOVE, 1934)

$$u_c(t) = \frac{1}{4\pi\rho v_c^3 r} \dot{M}\left(t - \frac{r}{v_c}\right) R^c_{\theta,\varphi},$$

where r is the distance, ρ is the density, v_c is the wave velocity and c stands for P or S depending upon the kind of wave considered. $R^c_{\theta,\varphi}$ represents the radiation pattern. Then the azimuth-averaged amplitude spectral density is given by

$$| \overline{\hat{u}_c(\omega)} | = \frac{\omega | \hat{M}(\omega) |}{4\pi\rho v_c^3 r} \overline{R^c_{\theta,\varphi}}, \tag{2}$$

where $\hat{M}(\omega)$ is the spectral density of $M(t)$ and $\overline{R^c_{\theta,\varphi}}$ is the average of $R^c_{\theta,\varphi}$ over the azimuths. The spectral density $| \overline{\hat{u}_c(\omega)} |$ in an infinite homogeneous medium can be related to the average amplitude spectral density $| \overline{\hat{U}_c(\omega)} |$ observed on the earth's surface by

$$| \overline{\hat{U}_c(\omega)} | = | C(\omega) | \exp\left[\frac{-\omega T_c}{2Q_c}\right] \frac{r}{R} g(\Delta, h) | \overline{\hat{u}_c(\omega)} |, \tag{3}$$

where T_c is the travel time, Q_c the path-averaged quality factor, and R the Earth's radius. In the above, $C(\omega)$ takes care of the effect of layerings including the free surface, and $g(\Delta, h)$ is the well-known factor which corrects for the ray spreading. The factor $g(\Delta, h)$ can be calculated from the travel time curve as a function of distance Δ and the source depth h by

$$g(\Delta, h) = \left[\frac{\rho_h v_{c,h}}{\rho_0 v_{c,0}} \frac{\sin i_h}{\sin \Delta} \frac{1}{\cos i_0} \left|\frac{di_h}{d\Delta}\right|\right]^{\frac{1}{2}},$$

where ρ_0, $v_{c,0}$ and i_0 are the density, the wave velocity and the angle of incidence at the surface respectively, and ρ_h, $v_{c,h}$ and i_h are the same quantities at the source depth h. Combining eqs. (2) and (3) we have

$$M_e(\omega) = \frac{4\pi\rho v_c^3 R \exp[\omega T_c/2Q_c]}{R^c_{\theta,\varphi} C(\omega) g(\Delta, h)} | \overline{\hat{U}_c(\omega)} |, \tag{4}$$

which gives the effective moment from the average amplitude spectral density at distance Δ. Since, in the present study, we will consider only shallow events ($h \approx 0$), and will be interested only in the order of magnitude estimate of $M_e(\omega)$, we make the following simplifications.

(1) $| C(\omega) | \approx 2$; i.e., only the free surface effect is considered.

(2) $T_P/Q_P \approx 1.25$ s and $T_S/Q_S \approx 4.87$ s. This follows from the result of CARPENTER and FLINN (1965) who suggested that, for short-period P waves, T_P/Q_P is almost constant at teleseismic distances. The result of KANAMORI (1967) supported this conclusion and gave $1.0 \text{ s} < T_P/Q_P < 1.5$ s which is used in the above estimate of T_P/Q_P. The estimate of T_S/Q_S is obtained from $T_P/Q_P = 1.25$ s and the relations $Q_P = 2.25\, Q_s$ (ANDERSON *et al.*, 1965) and $T_S = \sqrt{3} T_P$.

(3) $\overline{R^P_{\theta,\varphi}} = 0.52$, $\overline{R^S_{\theta,\varphi}} = 0.63$. These values are obtained by considering the average energy flux through a spherical shell around the source, i.e.,

$$\overline{R^P_{\theta,\varphi}} = \left[\frac{1}{4\pi}\int_0^{\pi} \sin\theta \left\{\int_0^{2\pi} \sin^2 2\theta \sin^2\varphi \, d\varphi\right\} d\theta\right]^{\frac{1}{2}},$$

$$\overline{R^S_{\theta,\varphi}} = \left[\frac{1}{4\pi}\int_0^{\pi} \sin\theta \left\{\int_0^{2\pi} \cos^2 2\theta \sin^2\varphi + \cos^2\theta \cos^2\varphi \, d\varphi\right\} d\theta\right]^{\frac{1}{2}}.$$

With these simplifications we have, substituting $\rho = 3.3$ g/cm^3, $v_P = 8.1$ km/s and $v_S = 4.7$ km/s into (4),

$$M_e(\omega) = 1.35 \times 10^{28} \frac{\exp[0.625\omega]}{g(\Delta, 0)} \mid \overline{\hat{U}_P(\omega)} \mid \text{dyne} \cdot \text{cm}, \quad (5)$$

$$M_e(\omega) = 2.17 \times 10^{27} \frac{\exp[2.435\omega]}{g(\Delta, 0)} \mid \overline{\hat{U}_S(\omega)} \mid \text{dyne} \cdot \text{cm}, \quad (6)$$

where $\mid \overline{\hat{U}_P(\omega)} \mid$ and $\mid \overline{\hat{U}_S(\omega)} \mid$ should be given in units of cm · s. These relations give the effective moment from $\mid \overline{\hat{U}_P(\omega)} \mid$ and $\mid \overline{\hat{U}_S(\omega)} \mid$ which are estimated from the body-wave magnitude through (1), if a certain reference distance Δ_r is chosen. In the present study, $\Delta_r = 80°$ is used but a different choice of Δ_r does not affect significantly the determination of the effective moment.

2.2. *Conversion of surface-wave magnitude to effective moment*

The surface-wave magnitude is directly proportional to the logarithm of the amplitude of the 20 s surface wave. The effective moment at 20 s is directly proportional to the amplitude. Thus if both the surface-wave magnitude and the effective moment at 20 s are known for a certain earthquake, the surface-wave magnitude for other earthquakes can be readily converted to the effective moment. As will be shown later, the effective moment at 20 s of the 1933 Sanriku earthquake (surface-wave magnitude ≈ 8.34) is estimated to be about 1.5×10^{28} dyne · cm. Using this result, we can convert the surface-wave magnitude M_S to the effective moment at 20 s M_e ($T = 20$ s) by

$$M_e(T = 20\text{ s}) = (1.5 \times 10^{28}) 10^{(M_S - 8.34)} \text{ dyne} \cdot \text{cm}. \quad (7)$$

2.3. *Long-period surface waves*

The spectral density of long-period surface waves can be converted to the effective moment by the use of the relations given by BEN-MENAHEM *et al.* (1970). With our definition of the effective moment $M_e(\omega)$, eqs. (1) and (2) of BEN-MENAHEM *et al.* (1970) can be rewritten as

$$M_e(\omega) = \frac{\mu\omega G_z \mid \overline{\hat{U}_z(\omega)} \mid}{s_R S_R + p_R P_R + i q_R Q_R} \quad \text{(for Rayleigh waves)}, \quad (8)$$

$$M_e(\omega) = \frac{\mu\omega G_\theta \mid \overline{\hat{U}_\theta(\omega)} \mid}{p_L P_L + i q_L Q_L} \quad \text{(for Love waves)}, \quad (9)$$

where G_z and G_θ are the diminution factors of Rayleigh and Love waves respectively as tabulated in table 6 of BEN-MENAHEM *et al.* (1970); $\mid \overline{\hat{U}_z(\omega)} \mid$ and $\mid \overline{\hat{U}_\theta(\omega)} \mid$ are the average amplitude spectral densities of vertical-component Rayleigh waves and transverse component of Love waves, respectively. The denominators in eqs. (8) and (9) can be calculated by use of tables 7 through 33 of BEN-MENAHEM *et al.* (1970) if the geometry of the force system is given. In our case, the detailed geometry of the source is not known. We therefore assume a certain force geometry and take the average over all azimuths. We assume a pure dip-slip faulting with a dip angle of 45°. Then we have

$$\mid p_L P_L + i q_L Q_L \mid = \pi^{-1} \mid P_L \mid,$$
$$\mid s_R S_R + p_R P_R + i q_R Q_R \mid = \tfrac{1}{2} \mid S_R \mid.$$

Since we assume the force geometry, no precise determination of the moment can be expected from a small number of determinations of $\mid \hat{U}_z(\omega) \mid$ or $\mid \hat{U}_\theta(\omega) \mid$. However it is hoped that averaging a large number of determinations of both $\mid \hat{U}_z(\omega) \mid$ and $\mid \hat{U}_\theta(\omega) \mid$, we may have a reasonably good estimate of $M_e(\omega)$. In the present paper we will place the source at a depth of 15 km, and will determine $M_e(\omega)$ at 50 s and 100 s. Using the numerical values of S_R and P_L given by BEN-MENAHEM *et al.* (1970), and combining n_R determinations of $\mid \hat{U}_z(\omega) \mid$ and n_L determinations of $\mid \hat{U}_\theta(z) \mid$, we can calculate $M_e(\omega)$ by

$$M_e(T = 100\text{ s}) = \frac{1}{n_R + n_L} (11.0\, n_L G_\theta \mid \hat{U}_\theta \mid + 4.9\, n_R G_z \mid \hat{U}_z \mid) \times 10^{26} \text{ dyne} \cdot \text{cm}, \quad (10)$$

$$M_e(T = 50\text{ s}) = \frac{1}{n_R + n_L} (15.0\, n_L G_\theta \mid \hat{U}_\theta \mid + 5.1\, n_R G_z \mid \hat{U}_z \mid) \times 10^{26} \text{ dyne} \cdot \text{cm}, \quad (11)$$

where $\mid \hat{U}_\theta \mid$ and $\mid \hat{U}_z \mid$ should be given in cm · sec.

2.4. *Tsunamis*

Tsunami data can be interpreted in terms of the volume V_T of displaced water at the tsunami source, which is equal to the volume of the displaced ocean bottom. If the displacement of the ocean bottom is caused by a shallow faulting, we may assume that

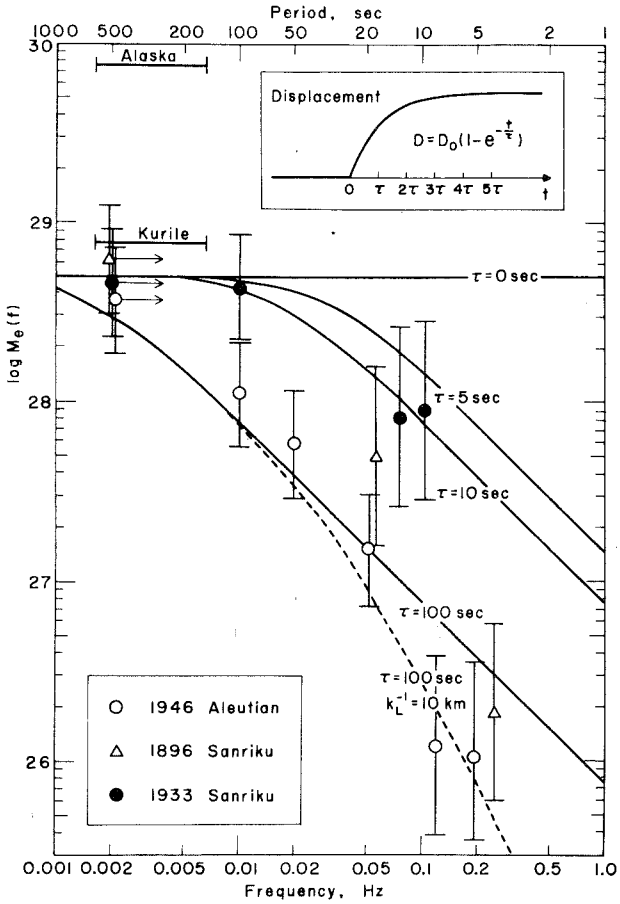

Fig. 3a. The effective moments as a function of frequency. The insert shows a dislocation function having a time constant τ introduced to fit the data. The solid curves give the effective moment corresponding to the dislocation functions with $\tau = 0$, 5, 10 and 100 s. The dashed curve is for a finite propagating source having a time constant of 100 s and a correlation length of 10 km.

$$V_T \approx (D_0 \sin\delta \sin\lambda)S,$$

where D_0 is the dislocation, δ is the dip angle, λ the slip angle and S is the area of the fault plane. Since the seismic moment M is equal to $\mu S D_0$, we have

$$M = \frac{\mu V_T}{\sin\delta \sin\lambda}. \qquad (12)$$

This is a very crude approximation. However, since the estimate of V_T is also subject to large uncertainty, a more involved assumption may not be meaningful at present.

The time constant of the displacement represented by tsunami data is not quite definite. According to KAJIURA (1970), the bottom deformations with a duration up to several minutes have approximately the same efficiency in tsunami generation.

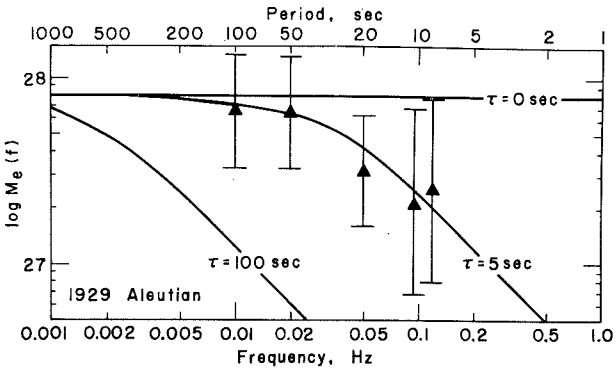

Fig. 3b. The effective moment as a function of frequency.

3. Results

In addition to the two tsunami earthquakes, two more earthquakes, the 1929 Aleutian islands earthquake and the 1933 Sanriku earthquake, are studied for the purpose of comparison. The results are summarized in figs. 3a and 3b and in table 7.

3.1. *Sanriku earthquake, March 2, 1933*

This earthquake is located beneath the axis of the Japan trench and is characterized by a normal faulting (KANAMORI, 1971a). RICHTER (1958) gave this event a magnitude of 8.9, the largest value ever reported. It was followed by a large tsunami which caused a devastating damage on the Sanriku coast. Unlike the 1896 event, the seismological data suggest that this event represents really a great earthquake. Recently, BRUNE and KING (1967) and KANAMORI (1971a) studied the 100 s surface waves excited by this earthquake.

The P-wave magnitude is determined as 8.16 at a period of $T = 9.4$ s (KANAMORI, 1971a). By using the chart given by GUTENBERG (1945) and RICHTER (1958), we then have, at a reference distance of 80°, $A/T \approx 1.8$ μm/s which gives an estimate of the spectral density $|\overline{U_P(\omega)}| = 0.16$ cm · s (eq. 1). Since at $\Delta_r = 80°$, $g(\Delta, 0) \approx 0.36$, eq. (5) gives an effective moment of 9.1×10^{27} dyne · cm. Similarly, the S-wave magnitude of 8.22 at a period of 12.6 s (KANAMORI, 1971a) can be interpreted as $|\overline{U_S(\omega)}| \approx 0.41$ cm · s at $\Delta_r = 80°$. Substituting this value into eq. (6), we have $M_e(\omega) \approx 8.3 \times 10^{27}$ dyne · cm. The effective moment at 100 s is identical to the seismic moment determined by 100 s

TABLE 1

Body-wave magnitude, Aleutian Islands earthquake, April 1, 1946

Station	Δ (°)	Azimuth (°)	A (μm)	T (s)	m_b
Belgrade	82.2	357.7	1.9 (P_H)	3.8	6.90
			3.4 (S_H)	6.0	6.65
Helwan	96.3	347.7	1.0 (P_H)	5.8	6.74
Göttingen	75.3	4.7	1.6 (P_Z)	4.0	6.45
			1.5 (P_H)	7.8	6.43
			3.0 (S_H)	10.5	6.26
Riverview	94.0	217.7	2.2 (P_Z)	5.8	6.78
Zürich	79.4	5.9	0.48 (P_H)	3.3	6.31
				Average P wave	6.60 (5.1 s)
				S wave	6.46 (8.3 s)

TABLE 2

Surface-wave magnitude, Aleutian Islands earthquake, April 1, 1946

Station	Δ (°)	Azimuth (°)	A (μm)	T (s)	M_s
Belgrade	82.2	357.7	100	20	7.18
Göttingen	75.3	4.7	128	20	7.22
Helwan	96.3	347.7	113	22	7.34
Hyderabad	92.1	303.1	434	20	7.90
Wellington	95.6	196.9	71	20	7.14
Zürich	79.4	5.9	143	20	7.30
				Average	7.35

Love and Rayleigh waves, which is 4.3×10^{28} dyne · cm (KANAMORI, 1971a).

HATORI (1967) determined by using the inverse refraction diagram the height of the sea-level disturbance at the margin of the tsunami source area on the basis of the inundation height observed along the coast. The usefulness of the inverse refraction diagram in estimating the bottom deformation at the source area has been demonstrated for the Niigata earthquake of 1964 (HATORI, 1965). From fig. 6 of HATORI (1967), the height of the sea-level disturbance averaged over the source area of 350×180 km^2 can be estimated to be 74 cm; the volume V_T of displaced water is therefore

$$V_T = 3.5 \times 1.8 \times 7.4 \times 10^{15} \text{ cm}^3 = 4.66 \times 10^{16} \text{ cm}^3 .$$

Since $\lambda = 90°$ and $\delta = 45°$ for this earthquake (KANAMORI, 1971a), eq. (12) gives a moment of 4.6×10^{28} dyne · cm, where 7×10^{11} dyne/cm^2 is used for the appropriate value of the rigidity. The effective moments thus determined are plotted in fig. 3a and listed in table 7.

The error bars in fig. 3a indicate the probable uncertainty in each determination. We assign the body-wave result one order of magnitude uncertainty. We assign the results obtained from 100 s surface waves and tsunamis uncertainties of factor 4. These uncertainties are assigned in view of the various assumptions made in the analysis and are not entirely objective. However, they are probably large enough to include the correct value within the range. As mentioned earlier, the tsunami data do not represent a single period; they are plotted at a period of 500 s since no efficient tsunami generation is expected by bottom displacements having a period longer than 500 s.

This earthquake has a surface-wave (20 s) magnitude of 8.34 (KANAMORI, 1971a). A smooth interpolation of the data in fig. 3a suggests that the effective moment at a period of 20 s is about 1.5×10^{28} dyne · cm. This observation leads to the relation (7) presented earlier.

3.2. *Aleutian Islands earthquake, April 1, 1946*

The body-wave magnitudes and the surface-wave magnitude determined in this study are listed in tables 1

TABLE 3

Spectral density of surface waves, Aleutian islands earthquake, April 1, 1946

Station	Instrument and component	Δ (°)	Azimuth (°)	$G_\theta \mid \hat{U}_\theta \mid$ (Love wave) (cm · s)		$G_z \mid \hat{U}_z \mid$ (Rayleigh wave) (cm · s)	
				$T = 100$ s	$T = 50$ s	$T = 100$ s	$T = 50$ s
Belgrade	Mainka (EW)	82.2	357.7	12.4	5.5	–	–
Florissant	Wood-Anderson (EW)	50.6	75.5	28.2	15.0	–	–
Göttingen	Wiechert (UD)	75.3	4.7	–	–	11.8	1.8
	Wiechert (NS, EW)	–	–	12.9	7.0	12.6	3.1
Helwan	Milne–Shaw (NS)	96.3	347.7	–	–	13.8	3.5
Riverview	Galitzin (UD, EW)	94.0	217.7	7.3	4.0	2.4	1.8
Wellington	Milne–Shaw (NS)	95.6	196.9	20.4	–	17.6	5.9
Zürich	Mainka (EW)	79.4	5.9	5.6	2.0	–	–
			Average	14.5	6.7	11.6	3.2

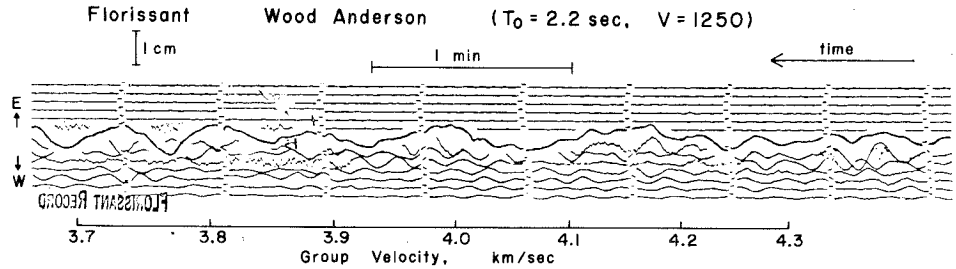

Fig. 4. The Wood–Anderson record of the 1946 Aleutian islands earthquake obtained at Florissant (38°48′ N, 90°22′ W). (By Courtesy of Prof. C. Kisslinger.)

and 2. The surface-wave magnitude of 7.35 may be compared with 7.4 given by GUTENBERG and RICHTER (1954). These magnitude values are converted to the effective moment at the respective periods (eqs. 5, 6, 7) and are plotted in fig. 3a. The spectral densities of 50 s and 100 s Love and Rayleigh waves are determined for several stations; the results are listed in table 3. In table 3, G_θ and G_z are the diminution factors as given in BEN-MENAHEM *et al.* (1970). The quantities $G_\theta \mid \hat{U}_\theta \mid$ and $G_z \mid \hat{U}_z \mid$ can therefore be considered as the spectral densities of the transverse component of Love waves and the vertical component of Rayleigh waves which would be observed at a distance of 90° on a non-attenuating Earth. When the spectral density of Rayleigh waves is determined on a horizontal component, it is multiplied by 1.4 to estimate approximate spectral density of the vertical component. For 100 s waves, the values of G_θ and G_z listed in table 6 of BEN-MENAHEM *et al.* (1970) are used. For 50 s waves, the experimental values of Q obtained by TSAI and AKI (1969) are used in computing G_θ and G_z. From fig. 3 of TSAI and AKI (1969), we take $Q = 170$ and $Q = 140$ for representative values for Love and Rayleigh waves, respectively. The effective moments are then computed by eqs. (10) and (11).

The effective moment at 100 s is significantly large compared with that determined at 20 s. This fact has been already pointed out by BRUNE and ENGEN (1969) who demonstrated the difference in terms of magnitude. This unusually large excitation of long-period surface waves may be best demonstrated by a Wood–Anderson ($T_0 = 2.2$ s, $V = 1250$) seismogram recorded at Florissant (fig. 4). The Love waves with periods up to 100 s are clearly recorded even by such short-period instruments.

The tsunami data are included only in an approximate manner. Although no direct observations on the height of the waves are made in the open sea, MACDONALD *et al.* (1947) suggested, on the basis of the wave height observed on the Hawaiian shores, that the height in the open sea probably did not exceed 2 ft from crest to trough. Although this value may have been "guessed" rather than estimated, it is unlikely to be wrong by a large factor. We will therefore use the value of 60 cm for the representative value of the crest-to-trough tsunami height in the open sea at a large distance.

If the wave length is long enough to justify the assumption of weakly dispersive propagation, the crest-to-trough amplitude, $\mid \eta \mid_{C-T}$, of the leading wave of tsunami at a large distance can be given by

$$\mid \eta \mid_{C-T} = (2\pi)^{-1} (\pi r)^{-\frac{1}{2}} (6/t)^{\frac{1}{2}} \mid T_P \mid_{C-T} V_T, \quad (13)$$

where r is the distance, t the travel time, V_T the volume of the displaced water at the tsunami source and $\mid T_P \mid_{C-T}$ is the crest-to-trough amplitude of a known function of time (see e.g. eq. 89 of KAJIURA, 1963). In the above, the length and the time are measured in units of H and $H/\sqrt{(gH)}$, where g is the acceleration of gravity and H is the water depth, and $\mid T_P \mid_{C-T} \approx 1.37$ (see fig. 3 of KAJIURA, 1963). It is also to be noted that the water depth is assumed to be uniform and that the above expression is valid for small values of $p_a = (6/t)^{\frac{1}{2}} a$, where a is the representative dimension of the tsunami source area (i.e., $a \approx$ radius of a circular tsunami souree area). In our case, the linear extent of the aftershock area is about 100 km (SYKES, 1971) and the travel time of the tsunami from the epicenter to Hawaii is about 16800 s. Assuming that the water depth is 5000 m, we have $p_a \approx 2$ which guarantees the use of eq. (13). Using the relation $r = t$, we can rewrite eq. (13) in the form

$$V_T \approx 3.4 \mid \eta \mid_{C-T} r H, \quad (14)$$

where V_T, $\mid \eta \mid_{C-T}$, r and H are either non-dimensional

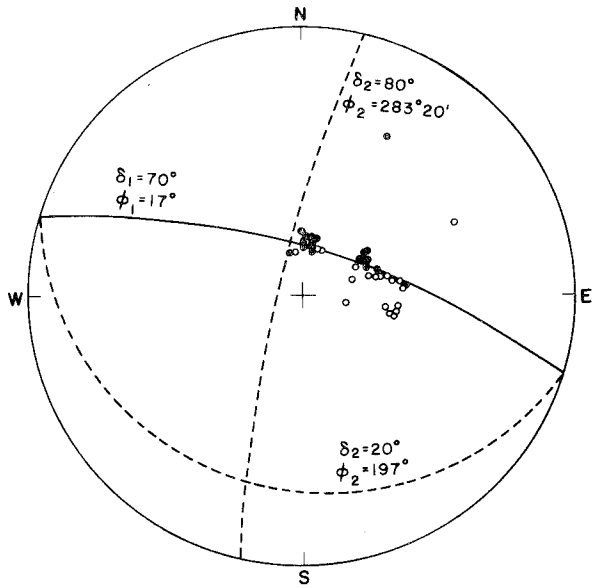

Fig. 5. The first motion of P waves on the lower half of the focal sphere plotted on the Wulff net. The open and the filled circles indicate the dilatational and the compressional first motions, respectively. Two possible pairs of nodal planes are shown. δ and φ are the dip angle and the dip direction, respectively. The first solution is defined by $\delta_1 = 70°$, $\varphi_1 = 17°$, $\delta_2 = 80°$ and $\varphi_2 = 283°20'$, and the second solution is defined by $\delta_1 = 70°$, $\varphi_1 = 17°$, $\delta_2 = 20°$ and $\varphi_2 = 197°$.

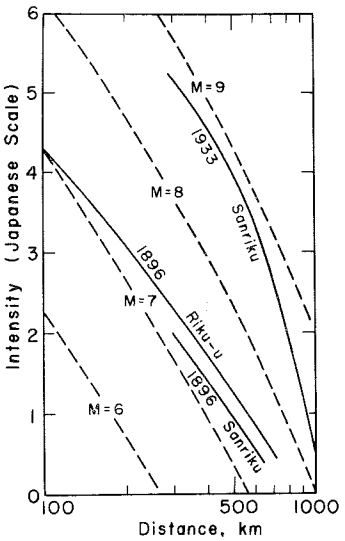

Fig. 6. The seismic intensity as a function of distance. The data of the three earthquakes, the 1933 Sanriku, the 1896 Sanriku and the 1896 Riku-u earthquakes, are according to the Japan Meteorological Agency. The dashed curves show empirical relations between the intensity and the distance for various magnitudes.

or actual physical parameters. Substituting $|\eta|_{C-T} =$ 60 cm, $r = 3700$ km and $H = 5$ km, we find $V_T = 3.75 \times 10^{16}$ cm^3. In order to obtain the moment from V_T the fault parameters δ and λ should be known. The first-motion data of this earthquake compiled by HODGSON and MILNE (1951) are shown on the Wulff net in fig. 5. HODGSON and MILNE (1951) discarded three "inconsistent" stations, and determined two P-wave nodal planes as: plane a, $\varphi = 292°$, $\delta = 85°$; plane b, $\varphi = 25°$, $\delta = 65°$; where φ is the dip direction and δ the dip angle. This solution represents predominantly a strike-slip faulting with some normal fault component. Fig. 5 shows, however, that many stations are distributed closely around a nodal line. It seems possible that, except for several "inconsistent" stations, the first-motion data can be made consistent with a variety of solutions from a pure normal fault to an almost strike-slip fault. Two such solutions are shown in fig. 5. If a solution with a large dip-slip component is chosen and the steep nodal plane ($\varphi = 17°$, $\delta = 70°$) is taken as the fault plane, it will favor the efficient generation of tsunamis by this earthquake. In view of the uncertainty in the fault geometry, we are forced to assume the values of δ and λ to estimate the moment. We assume $\delta = 45°$ and $\lambda = 90°$ and obtain $M = 3.7 \times 10^{28}$ dyne · cm.

The values of the moment determined at various periods are plotted in fig. 3a and listed in table 7. Fig. 3a clearly shows a very rapid increase of the effective moment as the period increases.

3.3. *Sanriku earthquake, June 15, 1896*

The seismological data are very incomplete for this event. However, several lines of evidence suggest that the excitation of seismic waves at short periods was not very large. Most convincing evidence is provided by the seismic intensity distribution as a function of distance shown in fig. 6. The seismic intensity scale used in this figure is the Japanese scale currently used by the Japan Meteorological Agency. Since a different intensity scale was used in 1896, it was converted to the present scale. In fig. 6, the data for the 1933 Sanriku earthquake and for the 1896 Riku-u earthquake are included. The dashed curves in fig. 6 represent the empirical curves

$$I = -0.317 - 4.6 \log \Delta - 0.00183\Delta + 2M$$

connecting the intensity I and the distance Δ with the magnitude M as a parameter. At a large distance

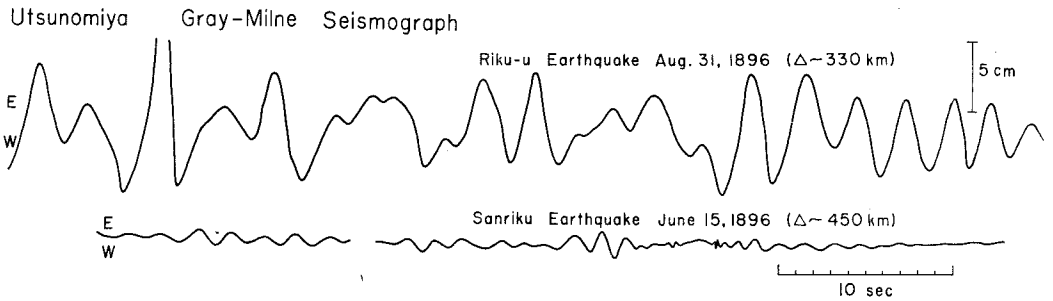

Fig. 7. The Gray–Milne record of the 1896 Sanriku (June 15) and the 1896 Riku-u (August 31) earthquakes obtained at Utsunomiya (36°33′ N, 139°52′ E). Only the EW component is shown.(By courtesy of the Japan Meteorological Agency.)

($\Delta \approx 600$ km), the difference of the intensity between the 1933 event and the 1896 event is about 2.40; this corresponds to a difference of 1.20 in the magnitude unit suggesting an amplitude ratio of about 16. At such a large distance, the longest period of the waves which give the maximum amplitude is about 4 s (YAMAGISHI, 1971); the above results indicate that at a period around 4 s the effective moment of the 1896 event is $\frac{1}{16}$ of that of the 1933 event. Since the effective moment of the 1933 event at a period of 4 s is estimated from fig. 3 to be about 3×10^{27} dyne · cm, the 1896 event may be given an effective moment of 1.88×10^{26} dyne · cm at this period.

The inefficient excitation of short-period seismic waves by the 1896 Sanriku earthquake can be further demonstrated by a record obtained at Utsunomiya by an old Gray–Milne type seismograph. Fig. 7 shows the seismogram of the 1896 Sanriku earthquake compared with that of the Riku-u earthquake on August 31 of the same year. Although the instrument constants of this type of seismograph found in literature are: horizontal component: free period = 3 s, magnification = 5; vertical component: free period = 3 s, magnification = 10, it is not certain whether the seismographs at Utsunomiya were adjusted precisely to this standard response in these early days of instrumental seismology. Since the Gray–Milne seismograph had a trigger-start recording system it is not possible to identify the phases reproduced in fig. 7. Nevertheless, comparison of the seismogram of the Sanriku earthquake with that of the Riku-u earthquake may give a crude measure of the size of the former relative to the latter event. Since these two events occurred only 2.5 months apart, the instrument response was unlikely to be changed drastically during this period. The amplitude of the Riku-u earthquake is much larger than that of the Sanriku earthquake even if the difference in the distance is allowed for. Since the Riku-u earthquake occurred on land, the macro-seismic data are very complete and, from the distribution of the intensity (see fig. 6), the magnitude of this earthquake can be estimated as about 7.5. On this ground it is confirmed that as far as the short-period waves (period $\approx$ 1 s) are concerned the 1896 Sanriku earthquake must have been a relatively small event of magnitude around 7.

Several seismological observatories in Italy were op-

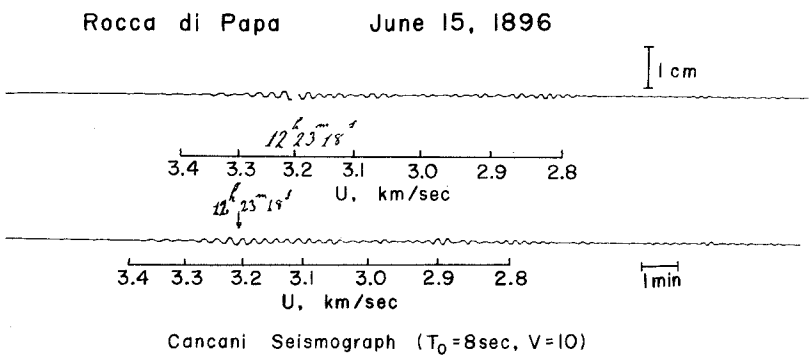

Fig. 8. The record of the 1896 Sanriku earthquake obtained by the Cancani seismograph ($T_0 = 8$ s, $V = 10$) at Rocca di Papa (41°45′ N, 12°43′ E). The upper trace shows the E (upward)–W (downward) component, and the lower trace shows the N (upward)–S (downward) component. (By courtesy of Prof. P. Caloi.)

TABLE 4

Body-wave magnitude, Aleutian Islands earthquake, March 7, 1929

Station	Δ (°)	Azimuth (°)	A (μm)		T (s)	m_b
Berkeley	35.1	93.4	48	(P_Z)	6.6	7.56
			25	(P_H)	6.4	7.49
			56	(S_H)	7.5	7.38
Göttingen	77.9	1.1	195	(P_Z)	9.4	8.07
			70	(P_H)	12.0	7.82
			90	(S_H)	11.0	7.91
Helsinki	68.8	352.9	50	(P_H)	9.0	7.85
Riverview	90.1	213.5	4.0	(P_H)	7.0	7.06
			52	(S_H)	10.0	7.60
Toledo	88.6	12.0	64	(P_H)	11.0	8.16
			174	(S_H)	15.0	8.06
Wellington	92.4	192.8	2.1	(P_H)	5.2	7.10
			23	(S_H)	10.0	7.31
Vienna	81.2	356.9	50	(P_H)	9.0	7.94
			85	(S_H)	10.0	7.83
				Average P wave		7.67 (8.4 s)
				S wave		7.68 (10.6 s)

TABLE 5

Surface-wave magnitude, Aleutian Islands earthquake, March 7, 1929

Station	Δ (°)	Azimuth (°)	A (μm)	T (s)	M_S
Berkeley	35.1	93.4	1300	20	7.68
Göttingen	77.9	1.1	244	20	7.54
Helsinki	68.8	352.9	440	23	7.65
Hyderabad	90.5	298.7	236	20	7.62
Lick	36.3	93.0	1550	18	7.82
Riverview	90.1	213.5	190	20	7.52
Toledo	88.6	12.0	610	19	8.05
Wellington	92.4	192.8	222	22	7.57
Vienna	81.2	356.9	296	20	7.63
				Average	7.68

erating reliable seismographs as early as 1896. Fortunately, the record obtained at Rocca di Papa is still preserved. This record which is reproduced in fig. 8 shows very clear 18 s surface waves with a group velocity of 3.0 to 3.3 km/s. This seismograph (Cancani) has a natural period of 8 s and a static magnification of 10. The surface-wave magnitude is determined from the combined horizontal amplitude as $M_S \approx 7.9$. Using eq. (7), we then have an effective moment of 5.0×10^{27} dyne · cm at 18 s.

The data on tsunami observed along the Sanriku coast are fairly complete. HATORI (1967) estimated, by using the inverse refraction diagram, the height of the sea-level disturbance at the margin of the tsunami source. From his fig. 6, the height of the sea-level disturbance averaged over the tsunami source area of 300×160 km^2 can be estimated to be 1.33 m, which leads to an estimate of the volume of the displaced water of 6.4×10^{16} cm^3. Assuming, as before, $\delta = 45°$ and $\lambda = 90°$, we have a moment of 6.3×10^{28} dyne · cm. These values are plotted in fig. 3a and listed in table 7. It is remarkable that the general trend is very similar to that for the 1946 Aleutian islands earthquake.

3.4. *Aleutian Islands earthquake, March 7, 1929*

This earthquake is located beneath the Aleutian trench (SYKES, 1971) and is given a magnitude of 8.1 by GUTENBERG and RICHTER (1954) who indicated a depth of 50 km. Because of the lack of near-station data, the depth cannot be determined precisely from the P time alone. Sykes (personal communication, 1972) suggested that any depth between 0 and 100 km can be made consistent with the P-wave data.

TABLE 6

Spectral density of surface waves, Aleutian Islands earthquake, March 7, 1929

Station	Instrument and component	Δ (°)	Azimuth (°)	$G_\theta \mid \hat{U}_\theta \mid$ (Love wave) (cm · s)		$G_z \mid \hat{U}_z \mid$ (Rayleigh wave) (cm · s)	
				$T = 100$ s	$T = 50$ s	$T = 100$ s	$T = 50$ s
Berkeley	Bosch–Omori (NS)	35.1	93.4	10.6	2.5	–	–
Göttingen	Wiechert (UD)	77.9	1.1	–	–	11.5	17.0
	Wiechert (NS, EW)	–	–	9.1	4.3	19.2	23.8
Helsinki	Mainka (UD)	68.8	352.9	–	–	14.5	25.0
	Mainka (NS)	–	–	–	–	11.9	14.3
Hyderabad	Milne–Shaw (NS)	90.5	298.7	10.5	8.8	–	–
Lisbon	Wiechert (NS)	89.0	16.0	–	–	8.0	3.4
Wellington	Milne–Shaw (EW)	92.4	192.8	2.0	2.1	–	–
Vienna	Wiechert (NS, EW)	81.2	356.9	1.6	0.6	8.1	3.8
			Average	6.8	3.7	12.2	14.6

TABLE 7

Effective moments (in units of 10^{26} dyne · cm)

Event	P wave	S wave	Surface wave			Tsunami
			20 s	50 s	100 s	
1896 Sanriku	—	1.9 ($T \approx 4$ s)	50 ($M_s = 7.90$)	—	—	630
1929 Aleutian	25 ($m_b = 7.67$, $T = 8.4$ s)	22 ($m_b = 7.68$, $T = 10.6$ s)	33 ($M_s = 7.68$)	66	67	—
1933 Sanriku	91 ($m_b = 8.16$, $T = 9.4$ s)	83 ($m_b = 8.22$, $T = 12.6$ s)	150 ($M_s = 8.34$)	—	430	460
1946 Aleutian	1.1 ($m_b = 6.60$, $T = 5.1$ s)	1.2 ($m_b = 6.46$, $T = 8.3$ s)	15 ($M_s = 7.35$)	58	110	370

The seismograms collected from several selected stations in the world show very large body waves with extremely sharp onsets. The results of body-wave magnitude determinations from both P and S waves are summarized in table 4. The amplitude of surface waves is not exceptionally large. The average surface-wave magnitude is 7.68 as listed in table 5. The spectral densities of 50 s and 100 s Love and Rayleigh waves are determined for several stations and are summarized in table 6. These magnitudes and the spectral densities are converted into the effective moment and plotted in fig. 3b (see also table 7). The trend of the variation of the effective moment as a function of frequency is very similar to that of the 1933 Sanriku earthquake, but, as a whole, the effective moment of the 1929 Aleutian islands earthquake is about $\frac{1}{6}$ of that of the 1933 Sanriku earthquake.

The first motion of the 1929 event is dilatational at all the teleseismic stations examined in the present study, suggesting a normal faulting (fig. 9). Although the number of data is not sufficient for the determination of the nodal planes, it is interesting to note that the nodal planes of a relatively large shock which occurred on July 29, 1965, in the vicinity of the epicenter of the 1929 event (STAUDER, 1968b) are consistent with the first-motion data of the 1929 event (fig. 9). STAUDER (1968b) showed that the earthquakes along the axis of the Aleutian trench can be represented very systematically by a normal faulting with the strike more or less parallel to the trench axis. The spatial proximity of the 1929 event to these normal-fault earthquakes suggests that the 1929 event is very likely to represent a normal faulting as shown in fig. 9. Thus this earthquake is, in many ways, very similar to the 1933 Sanriku earthquake, but of considerably smaller magnitude.

4. Interpretation

The results summarized in figs. 3a and 3b clearly show that the two tsunami earthquakes have effective moments which strongly depend on the period. This dependence can be interpreted in terms of a dislocation of a type

$$D(t;\tau) = D_0(1-e^{-t/\tau}),$$

which gives the effective moment in the form

$$M_e(\omega) = M_0\{1+(\omega\tau)^2\}^{-\frac{1}{2}}. \qquad (15)$$

The solid curves in fig. 3a are the curves for $\tau = 0$, 5, 10 and 100 s with $M_0 = 5\times10^{28}$ dyne · cm. The data on the "ordinary" event, the 1933 Sanriku earthquake, can be fitted by a curve with $\tau = 10$ s, while the two tsunami earthquakes require a time constant of more than 100 s. In view of the large uncertainty in the determination of the effective moment, the numerical values

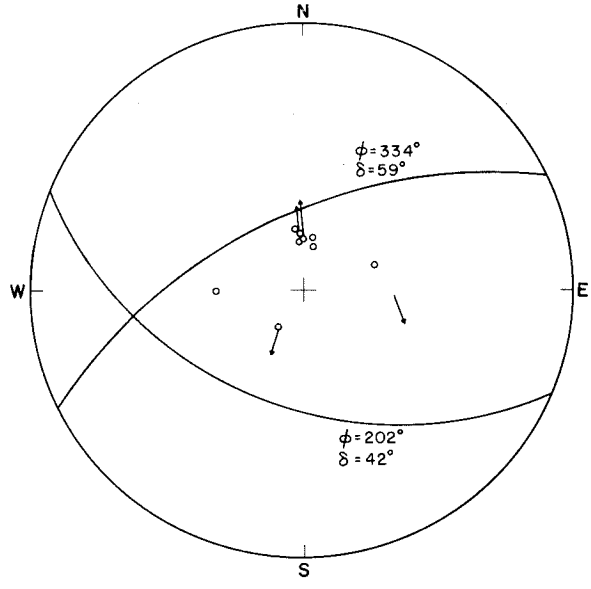

Fig. 9. The first motion of P waves on the lower half of the focal sphere plotted on the Wulff net. All the stations show dilatational first motions (open circle). The arrows show the polarization angles of S waves. The nodal planes determined for an earthquake on July 29, 1965 which occurred about 100 km west of the 1929 event are shown (STAUDER, 1968b).

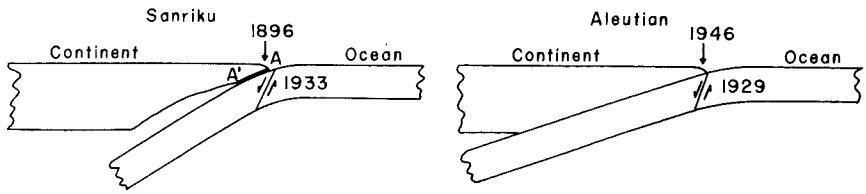

Fig. 10. Schematic models showing the relation between the normal-fault earthquake and the tsunami earthquake.

may not have much significance. It is emphasized that the tsunami earthquakes have a time constant of the order of 100 s while the "ordinary" earthquake is characterized by a more or less instantaneous dislocation. The data on the 1929 Aleutian islands earthquake can be fitted by a curve with $\tau = 5$ s (fig. 3b). As before, this result should be considered as indicating an instantaneous dislocation.

In the above interpretation, we assumed a point source, which is of course a crude approximation, particularly at short periods. In general, the finiteness of the source suppresses the short-period waves. HASKELL (1966) and AKI (1967) introduced a parameter k_L^{-1}, called correlation length, to express a partially coherent rupture propagation. Radiation of short-period waves from such a finite propagating fault (rupture velocity v) is suppressed according to $\{1+(\omega k_L^{-1} v^{-1})^2\}^{-\frac{1}{2}}$ at an "average" azimuth of $\frac{1}{2}\pi$ measured from the rupture direction. Including the finiteness effect, we then have instead of eq. (15)

$$M_e = M_0[\{1+(\omega\tau)^2\}\{1+(\omega k_L^{-1} v^{-1})^2\}]^{-\frac{1}{2}}. \quad (16)$$

The dotted curve in fig. 3a gives the effective moment with $\tau = 100$ s, $k_L^{-1} = 10$ km and $v = 2.5$ km/s; this curve fits better the short-period data of the tsunami earthquakes.

Fig. 3a includes the results obtained for two large earthquakes, the Kurile islands earthquake of 1963 and the Alaska earthquake of 1964, for which the effective moment has been shown to be constant over a fairly wide spectral range, 150 to 600 s (KANAMORI, 1970a, b; ABE, 1970). In fact, this constancy of the effective moment has been the basis of the ordinary concept of earthquake source that the source dislocation takes place within a relatively short time. Even for an extremely large earthquake like the Kamchatka earthquake of 1952 BEN-MENAHEM and TOKSÖZ (1963) suggested a time constant of about 30 s. For smaller earthquakes, smaller time constants seem to be more natural. Thus in the light of this ordinary concept of earthquake source, the time constant of the order of 100 s required for the tsunami earthquakes whose source dimension is not exceptionally large is certainly anomalous. It may be argued that the dislocation model may not be adequate for deformations having such a large time constant. However, the conclusion that the tsunami earthquakes involved a deformation having an extremely long duration seems unavoidable, whatever type of deformation it may have been.

5. Discussions

The 1896 Sanriku earthquake and the 1946 Aleutian islands earthquake are probably the only two great tsunami earthquakes since the dawn of instrumental seismology. It is interesting to note that these anomalous events occurred in the regions of unique seismicity. Unique in the Aleutian and the Sanriku regions are the large normal-fault earthquakes along the trench axis. These are probably the only two regions in the world where such major seismic activity exists along the trench axis. The Sanriku earthquake of 1933 is the largest of such normal-fault earthquakes ever reported. This earthquake which suggests a fracture over the entire thickness of the lithosphere can be considered to be a result of decoupling between the oceanic and the continental lithospheres at the interface AA′ (see fig. 10); owing to this decoupling, the gravitational pull exerted by the dense downgoing lithosphere can be transmitted to the source region of the 1933 event to cause such a normal faulting. Such decoupling may have been caused by prolonged frictional heating and subsequent partial melting (KANAMORI, 1971b). Thus such normal-fault earthquakes may imply the presence of a weak zone along the inner margin of the trench. It is in this part of the trench that the tsunami earthquake of 1896 occurred (see figs. 1 and 10). The structure here can be modeled by a thin lithosphere underlain by the weak zone along AA′. This structure offers an explanation,

though a speculative one, for such a "slow" earthquake. The thin lithosphere above the weak zone may break off, probably owing to its own weight, by a brittle fracture followed by a more or less creep-like deformation of the visco-elastic weak zone. This creep-like deformation cannot be felt as an ordinary earthquake, but it can generate tsunamis. The tsunami earthquake may be a manifestation of such a brittle fracture in the thin lithosphere followed by the creep-like deformation of the weak zone.

The situation is slightly different along the Aleutians. In the Sanriku region the decoupling at the interface AA′ is evidenced by the lack of great thrust earthquakes between the trench and the coast line. Along the Aleutians, however, great earthquakes frequently occur between the trench and the islands. Thus there is no evidence for complete decoupling at the interface. However, the occurrence of considerably large normal-fault earthquakes such as the ones on March 30, 1965 (STAUDER, 1968a; ABE, 1972) and on March 7, 1929 suggest a local decoupling of the lithospheres. ABE (1972) suggested that the earthquake on March 30, 1965, represents a fracture that cuts through the oceanic lithosphere. He considers that the preceding large thrust earthquake of February 4, 1965, caused a temporary decoupling. The 1929 earthquake has a seismic moment twice as large as that of the earthquake on March 30, 1965. It may also represent a large scale fracture as shown in fig. 10. The spatial relation between the 1946 tsunami earthquake and the 1929 earthquake may therefore be quite similar to that between the two Sanriku earthquakes, although the two earthquakes in the Aleutians are about 500 km apart along the trench. Thus, we may postulate, for the 1946 earthquake, a mechanism similar to that considered for the 1896 Sanriku earthquake. The mechanism proposed here, however, is speculative, and it does not rule out other mechanisms such as large submarine slumps (GUTENBERG, 1939; SYKES, 1971).

If the extensive weak zone exists along the inner margins of the trenches, then a large secular vertical displacement of the ocean bottom may be expected. Precise determinations of the change of the ocean depth, as a function of time, may therefore help to evaluate the above possibility.

The 1896 Sanriku earthquake was followed by a large number of aftershocks (OMORI, 1900). Some of the larger shocks are listed in RICHTER (1958, p. 560) and plotted in fig. 1. These aftershocks, which are fairly large as earthquakes but did not generate large tsunamis, can be considered to represent readjustment of the stress in the thin lithosphere that broke off and settled at the time of the 1896 shock. The 1946 Aleutian islands earthquake was also followed by about 15 relatively large aftershocks (SYKES, 1971), but none of them generated large tsunamis.

BRUNE and ENGEN (1969) suggested that 100 s wave data should be used as a diagnostic aid in estimating the tsunami potential of an earthquake. Figs. 3a and 3b evidently suggest that, in addition to the 100 s wave data, inclusion of seismic-wave data over a wider frequency range will help in estimating more precisely the tsunami potential. A large effective moment at long-periods obviously leads to a high tsunami potential. A relatively low effective moment at long-periods may also indicate a high tsunami potential if the slope of the M_e–f curve is large enough to suggest a moment larger than 10^{28} dyne · cm at zero-frequency. Since the determination of the effective moment at different periods can be easily made by the conventional methods through eqs. (5), (6), (7), (10) and (11), this scheme for estimating the tsunami potential could be incorporated in the routine tsunami warning system.

6. Conclusions

The two tsunami earthquakes, the 1896 Sanriku and the 1946 Aleutian islands earthquakes, are very similar to each other with respect to the excitations of seismic waves at different periods. Despite the relatively small earthquake magnitude, these two earthquakes have, at long periods, a large effective moment of about 5×10^{28} dyne · cm which compares with the values for major earthquakes. If the faulting of these earthquakes has a large dip-slip component, this value is large enough for generating such devastating tsunamis. Such unusual excitation requires a deformation at the source having a time constant of the order of 100 s. A weak zone formed as a result of the interaction between the oceanic and the continental lithospheres at the inner margins of the trenches may be responsible for such a slow deformation.

Determinations of the effective moment at various periods may offer a powerful diagnostic aid in estimating the tsunami potential of earthquakes.

Acknowledgments

This paper was stimulated by discussions with Professor Kinjiro Kajiura in connection with the striking difference between the 1896 and the 1933 Sanriku earthquakes. Professor Kajiura made many valuable suggestions on the analysis of tsunami data. Professor Lynn Sykes kindly sent me a preprint of his paper from which I greatly benefited. He also informed me of the uncertainty in the depth of the 1929 earthquake in the Aleutians. Conversations with Professor Kazuaki Nakamura were very helpful in increasing my knowledge on the possibility of sea-bottom slumps. Dr. Hideo Watanabe kindly provided me with useful information on the seismographs and the intensity scale used in Japan in 1896. To these colleagues I express my sincere thanks. The seismograms used in the present study were kindly supplied by many seismological observatories in the world and of the Japan Meteorological Agency, the names of which, however, are too numerous to mention here. I would like to express my sincere thanks to these observatories. The assistance by Miss Tatoko Hirasawa throughout this study is gratefully acknowledged.

References

ABE, K. (1970), Phys. Earth Planet. Interiors **4**, 49–61.
ABE, K. (1972), Phys. Earth Planet. Interiors **5**, 190–198.
ADAMS, W. M. (1971), EOS Trans. Am. Geophys. Union **52**, 250.
AKI, K. (1967), J. Geophys. Res. **72**, 1217–1231.
ANDERSON, D. L., A. BEN-MENAHEM and C. B. ARCHAMBEAU (1965), J. Geophys. Res. **70**, 1441–1448.
BEN-MENAHEM, A. and M. N. TOKSÖZ (1963), J. Geophys. Res. **68**, 5207–5222.
BEN-MENAHEM, A., M. ROSENMAN and D. G. HARKRIDER (1970), Bull. Seismol. Soc. Am. **60**, 1337–1387.
BRUNE, J. N. and G. R. ENGEN (1969), Bull. Seismol. Soc. Am. **59**, 923–933.
BRUNE, J. N. and C. Y. KING (1967), Bull. Seismol. Soc. Am. **57**, 1355–1365.
CARPENTER, E. W. and E. A. FLINN (1965), Nature **207**, 745–746.
GREEN, G. K. (1946), Trans. Am. Geophys. Union **27**, 490–500.
GUTENBERG, B. (1939), Bull. Seismol. Soc. Am. **29**, 517–526.
GUTENBERG, B. (1945), Bull. Seismol. Soc. Am. **35**, 117–130.
GUTENBERG, B. and C. F. RICHTER (1954), *Seismicity of the Earth*, 2nd ed. (Princeton University Press, Princeton, N.J.) 310 pp.
HASKELL, N. (1966), Bull. Seismol. Soc. Am. **56**, 125–140.
HATORI, T. (1965), Bull. Earthquake Res. Inst. Tokyo Univ. **43**, 129–148.
HATORI, T. (1967), J. Seismol. Soc. Japan **20**, 164–170 (in Japanese).
HODGSON, J. H. and W. G. MILNE (1951), Bull. Seismol. Soc. Am. **41**, 221–242.
IKI, T. (1896), Rept. Imperial Earthquake Invest. Comm. **11**, 5–34 (in Japanese).
IMAMURA, A. (1899), Rept. Imperial Earthquake Invest. Comm. **29**, 17–32 (in Japanese).
IMAMURA, A. (1937), *Theoretical and applied seismology* (Maruzen, Tokyo) 358 pp.
KAJIURA, K. (1963), Bull. Earthquake Res. Inst. Tokyo Univ. **41**, 535–571.
KAJIURA, K. (1970), Bull. Earthquake Res. Inst. Tokyo Univ. **48**, 835–869.
KANAMORI, H. (1967), Bull. Earthquake Res. Inst. Tokyo Univ. **45**, 299–312.
KANAMORI, H. (1970a), J. Geophys. Res. **75**, 5011–5027.
KANAMORI, H. (1970b), J. Geophys. Res. **75**, 5029–5040.
KANAMORI, H. (1971a), Phys. Earth Planet. Interiors **4**, 289–300.
KANAMORI, H. (1971b), Tectonophys. **12**, 187–198.
LOVE, A. E. H. (1934), *A treatise on the mathematical theory of elasticity*, 4th ed. (Cambridge Univ. Press, Cambridge) 643 pp.
MACDONALD, G. A., F. P. SHEPARD and D. C. COX (1947), Pacific Sci. **1**, 21–37.
OMORI, F. (1900), Rept. Imperial Earthquake Invest. Comm. **34**, 5–79 (in Japanese).
RICHTER, C. F. (1958), *Elementary seismology* (Freeman, San Francisco, Calif.) 768 pp.
STAUDER, W. (1968a), J. Geophys. Res. **73**, 3847–3858.
STAUDER, W. (1968b), J. Geophys. Res. **73**, 7693–7701.
SYKES, L. R. (1971), J. Geophys. Res. **76**, 8021–8041.
TSAI, Y. B. and K. AKI (1969), Bull. Seismol. Soc. Am. **59**, 275–287.
YAMAGISHI, N. (1971), Tech. Rept. Japan Meteorol. Agency **76**, 35–38 (in Japanese).